Electronic Supplementary Material (ESI) for Physical Chemistry Chemical Physics.

Supporting Information

Valence- and Element-dependent Water Oxidation Behaviors: *in-situ* X-ray Diffraction, Absorption and Electrochemical Impedance Spectroscopies

*Chia-Shuo Hsu,[1§] Nian-Tzu Suen,[1§] Ying-Ya Hsu,[2§] Hsuan-Yu Lin,[1] Ching-Wei Tung,[1] Yen-Fa Liao,[3] Ting-Shan Chan,[3] Hwo-Shuenn Sheu,[3] San-Yuan Chen[4] and Hao Ming Chen[1]**

[1]Department of Chemistry, National Taiwan University, Taipei 106, Taiwan

[2]Program for Science and Technology of Accelerator Light Source, National Chiao Tung University, Hsinchu 300

[3]National Synchrotron Radiation Research Center, Hsinchu 300, Taiwan

[4]Department of Materials Science and Engineering, National Chiao Tung University, Hsinchu 300, Taiwan

[§] Authors contributed equally to the work

Experimental Section

Materials and samples preparation. Iron acetylacetonate, potassium hydroxide, and benzyl ether were purchased from ACROS. Cobalt 2,4-pentanedionate, γ-ferric oxyhydroxide, and nickel 2,4-pentanedionate were purchased from Alfa. Cobalt(II) hydroxide and nickel(II) hydroxide were purchased from Aldrich, while zinc(II) hydroxide and zinc acetylacetonate hydrate were purchased from Strem Chemicals and Fisher, respectively. Sodium oleate, iron chloride hexahydrate, and oleic acid were purchased from SHOWA. In terms of synthesis spinel-type MFe$_2$O$_4$, we used standard Schlenk line technique under nitrogen atmosphere. In typical synthesis of Fe ferrite nanocubes, iron acetylacetonate (0.706 g, 2 mmole) and oleic acid (2.258g, 8 mmole) were mixed in 20 mL benzyl ether. In the cases of synthesis of Co, Ni, and Zn ferrite, 0.66 mmole M(acac)$_2$ and Fe(acac)$_3$ were mixed with 8 mmole oleic acid in 20 mL benzyl ether. The solution was degassed for 30 min first and heated to 270 ℃ (with a ramping rate of 10 ℃/min) under magnetic stirring, this solution was maintained at this temperature for another 5 hours. In all cases, the final dark products were cooled to room temperature, the ferrites were washed with toluene after cooling this solution to room temperature. The product was then centrifuged at 8000 rpm for 20 minutes to precipitate the magnetite nanocubes, the separated precipitate was washed again using alcohol to obtain final product for further characterization.

Characterization. The morphology of the catalysts was studied by using transmission electron microscopy (TEM) including both JEOL JEM-2100F microscope with field-emission gun source

and Hitachi H-7650. For the sample preparation of TEM, the catalysts were dispersed in toluene and then dropped onto a copper grid and evaporating at room temperature in atmosphere. Oxygen gas evolution was measured in real-time by a Gas chromatography (Agilent 7890B) with TCD (thermal conductivity detector), and X-ray absorption measurements were conducted by using synchrotron radiation at beam line 01C1 and 17C of NSRRC in Taiwan.

Electrochemical Measurement. All electrochemical characterization were investigated by either CHI-704E (CHI-potentiostat) or BioLogic VSP in a standard three-electrode configuration cell using rotating disk electrode (RDE) voltammetry with a glass-carbon disk at 2000 rpm (PINE:AFE3T050GC , 5 mm in diameter, area: 0.196 cm^2) as the working electrode, Ag/AgCl electrode and platinum plate acted as reference and counter electrodes, respectively. In the case of working electrode preparation, the electrocatalysts were dispersed in ethanol (1mg/mL) and then dropped (20 μL) onto glassy carbon. The catalyst-loaded electrode was covered by 1% Nafion solution of 20 μL and dried in room temperature. Electrochemical experiments and Impedance spectra were performed in an electrolyte of 0.5 M KOH solution, all potentials were corrected with ohmic potential losses (R_u) that arose from the solution resistance. The calibrated potential with respect to reversible hydrogen electrode (RHE) was shown below:

$E_{RHE} = E_{ref} + 0.05916*pH-i*R_u$

Ex-situ X-ray absorption studies. For preparing *ex-situ* X-ray absorption sample, we dispersed electrocatalysts in toluene (5mg/mL) by sonication for 1 hour to obtain a homogeneous colloidal. Then 50 μL of colloidal was dropped onto FTO substrate (F:SnO_2, Tec15,~10Ω) which was

ultrasonically cleaned in acetone, 2-propanol, and deionized water sequentially. The electrode was dried at vacuum and heated at 300 ℃ for 3 hours to achieve better junction between FTO and electrocatalysts. All of the electrocatalysts (after OER) were prepared under an applied potential of 1.66 V (vs RHE) for 10 hrs and sent into specimen chamber within 1 min, X-ray absorption spectra of O K-edge were collected through total electron yield at beamline 20A of NSRRC in Taiwan.

In-situ X-ray diffraction studies. In-situ X-ray diffraction studies were collected by employing synchrotron radiation light source at beamline 01C2 of NSRRC in Taiwan, incident X-rays with a wavelength of 1.033210 Å (12 KeV) and a Si (111) triangular crystal monochromator was employed to obtain distinguishing scattering rings in an optimized situation. The catalyst-loaded FTO electrodes were operated in a handmade Teflon cell with a kapton polyimide film (DuPont) X-ray window. The detailed experimental setup can be referred to our previous work (ref 18). The diffraction angles were calibrated by utilizing Bragg positions of CeO_2 standard, and integrating a cake-type pattern through program of GSAS II was used to obtain corresponding one-dimensional powder diffraction profile.

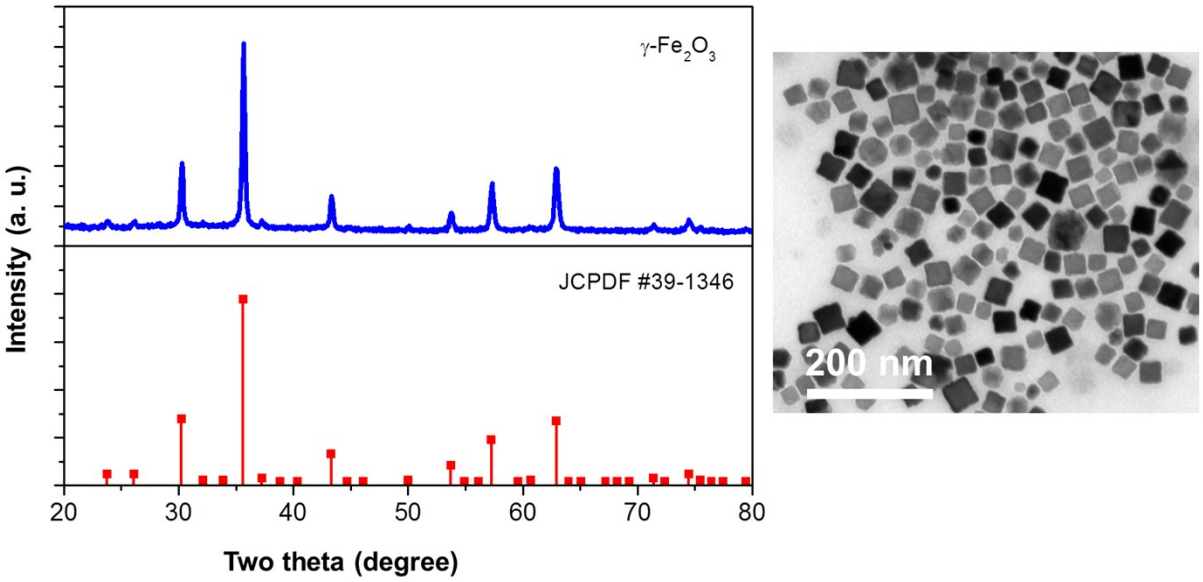

Figure S1. XRD spectrum and corresponding TEM image of γ-Fe_2O_3 reference sample.

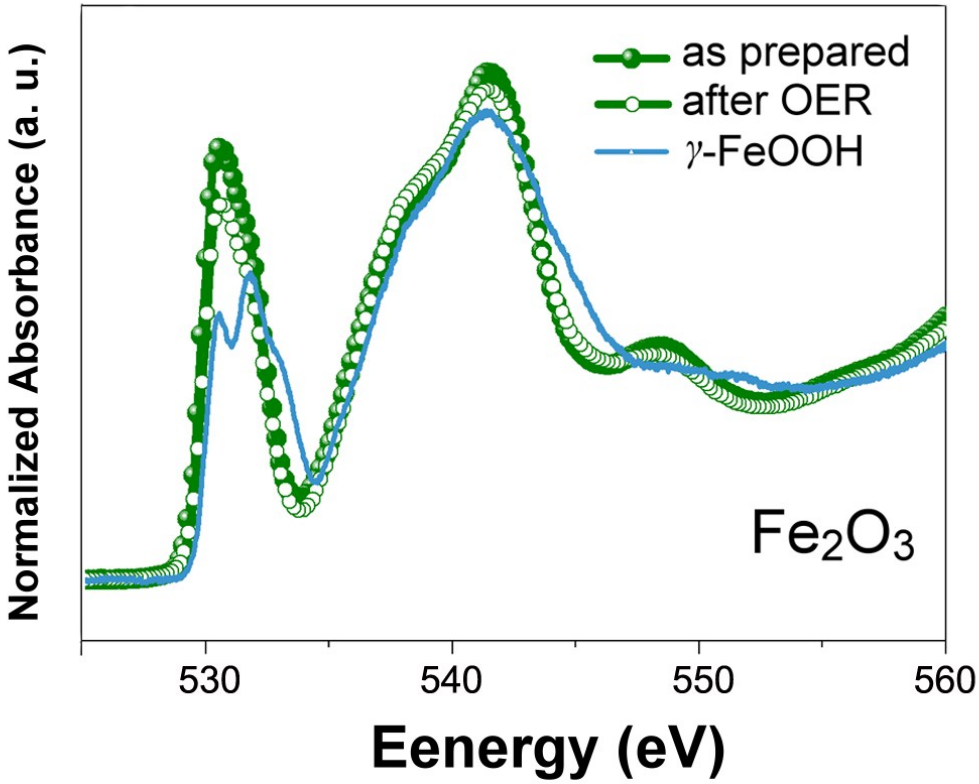
Normalized Absorbance (a. u.)
as prepared
after OER
γ-FeOOH
Fe2O3
530
540
550
560
Eenergy (eV)

Figure S2. XANES spectra of O *K*-edge for γ-Fe_2O_3.

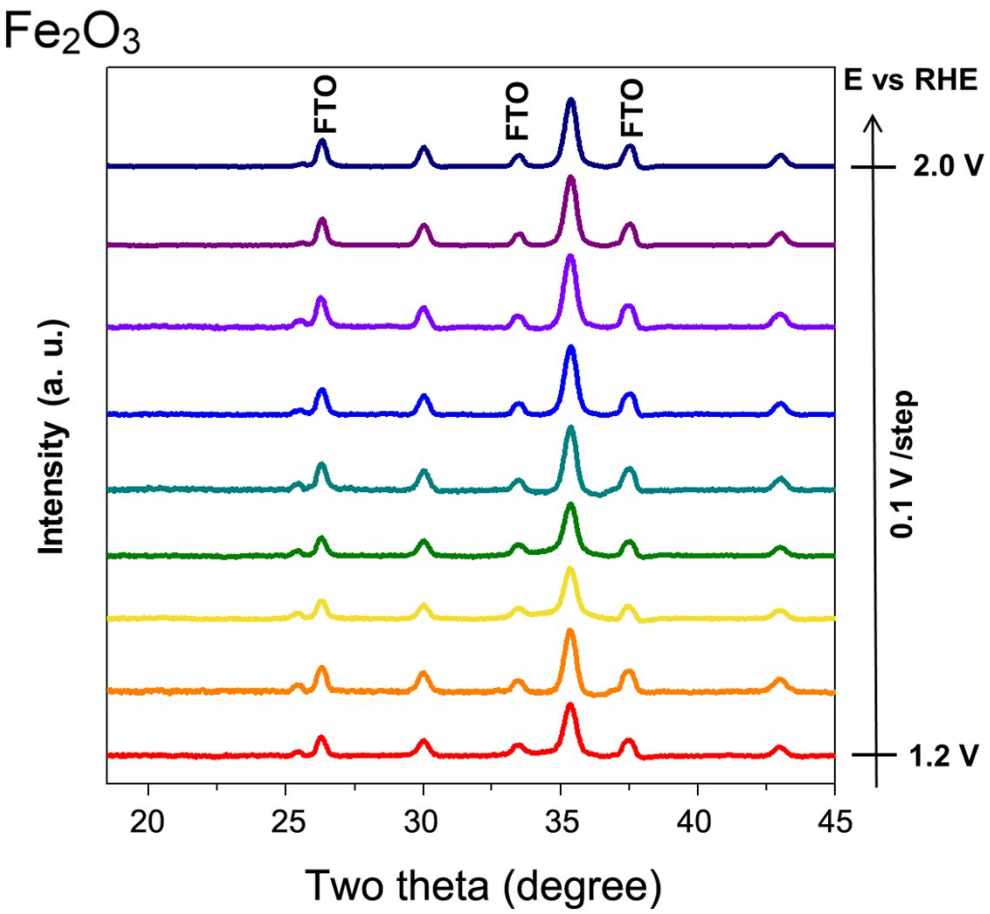

Figure S3. *In-situ* XRD spectra of γ-Fe_2O_3 sample, an electrolyte of 0.5 M KOH was employed with a potential range from 1.2 to 2.0 V vs RHE.

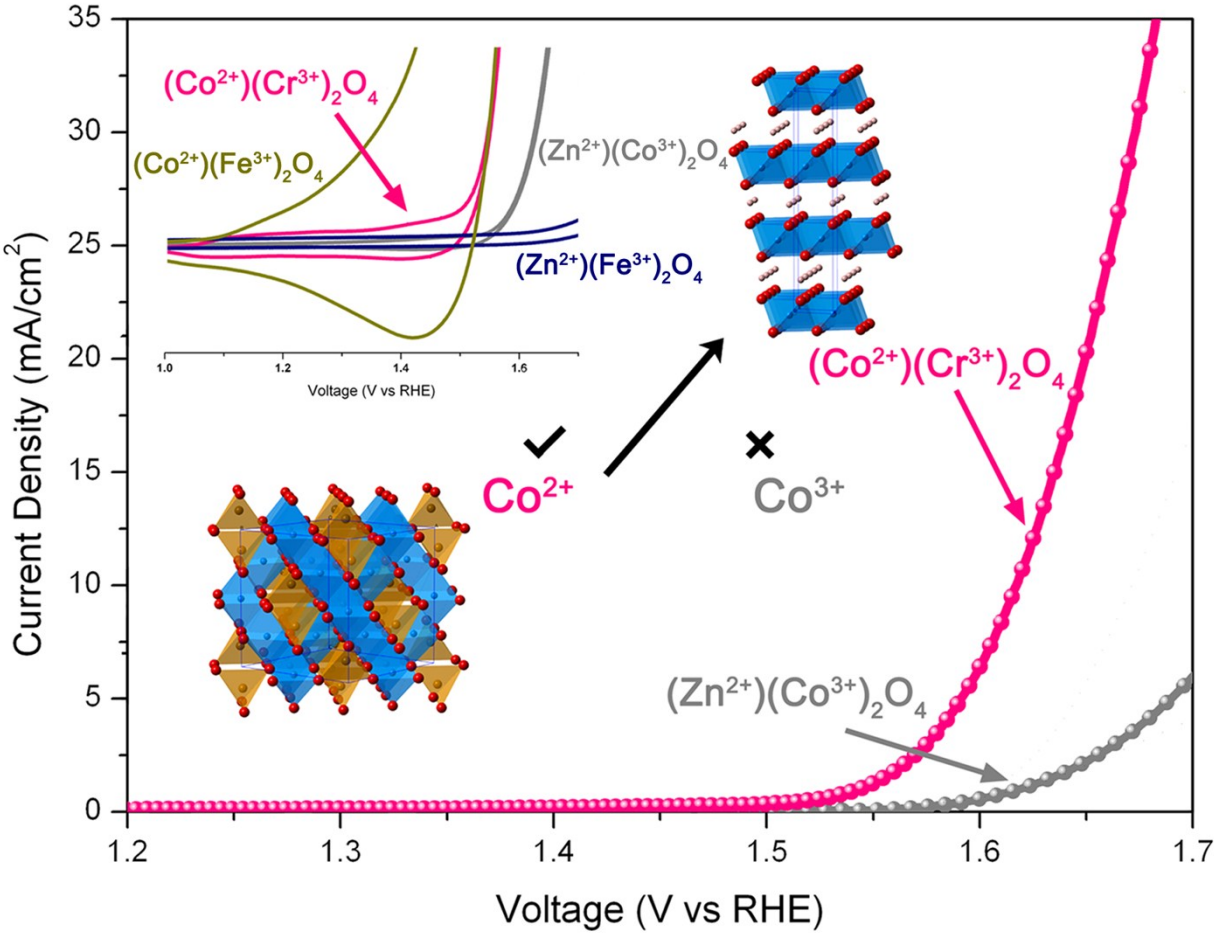

Figure S4. Electrochemical performance for $ZnCo_2O_4$ and $CoCr_2O_4$, the OER polarization curves were performed upon a GC-RDE system in alkaline electrolyte (0.5M KOH; pH~13.6). Insert: Cyclic voltammogram of $ZnCo_2O_4$, $CoCr_2O_4$, $ZnFe_2O_4$, and $CoFe_2O_4$.

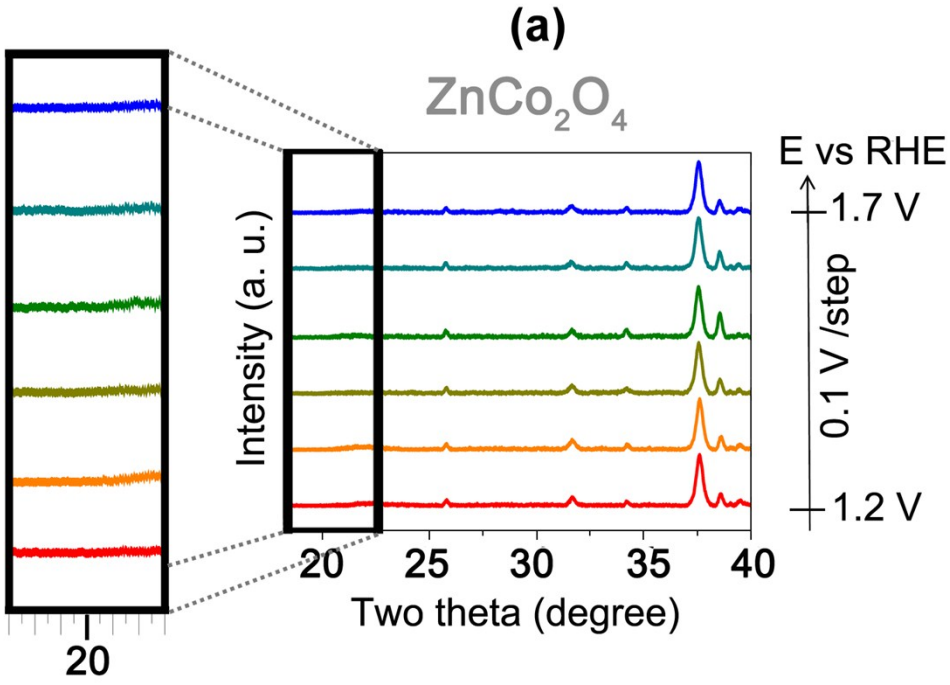
(a)
ZnCo2O4
E vs RHE
1.7 V
0.1 V /step
1.2 V
Intensity (a. u.)
20
25
30
35
40
Two theta (degree)
20

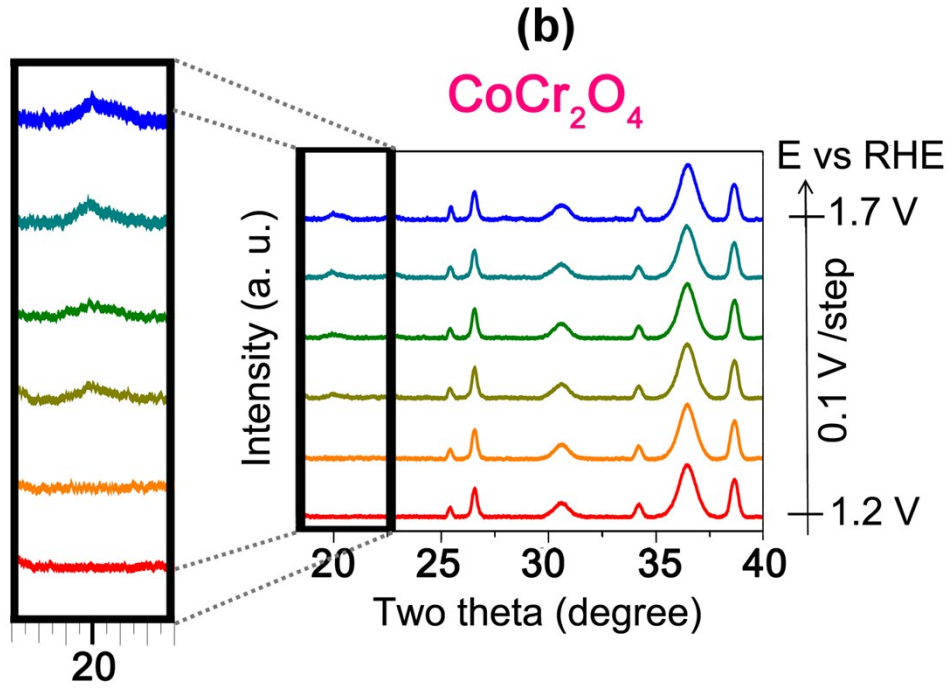
(b)
CoCr2O4
E vs RHE
1.7 V
0.1 V /step
1.2 V
Intensity (a. u.)
20
25
30
35
40
Two theta (degree)
20

Figure S5. *In-situ* XRD spectra of $ZnCo_2O_4$ and $CoCr_2O_4$ samples, a KOH electrolyte of 0.5 M was employed and all measurements with a potential range from 1.2 to 1.7 V vs RHE were operated potentiostatically.

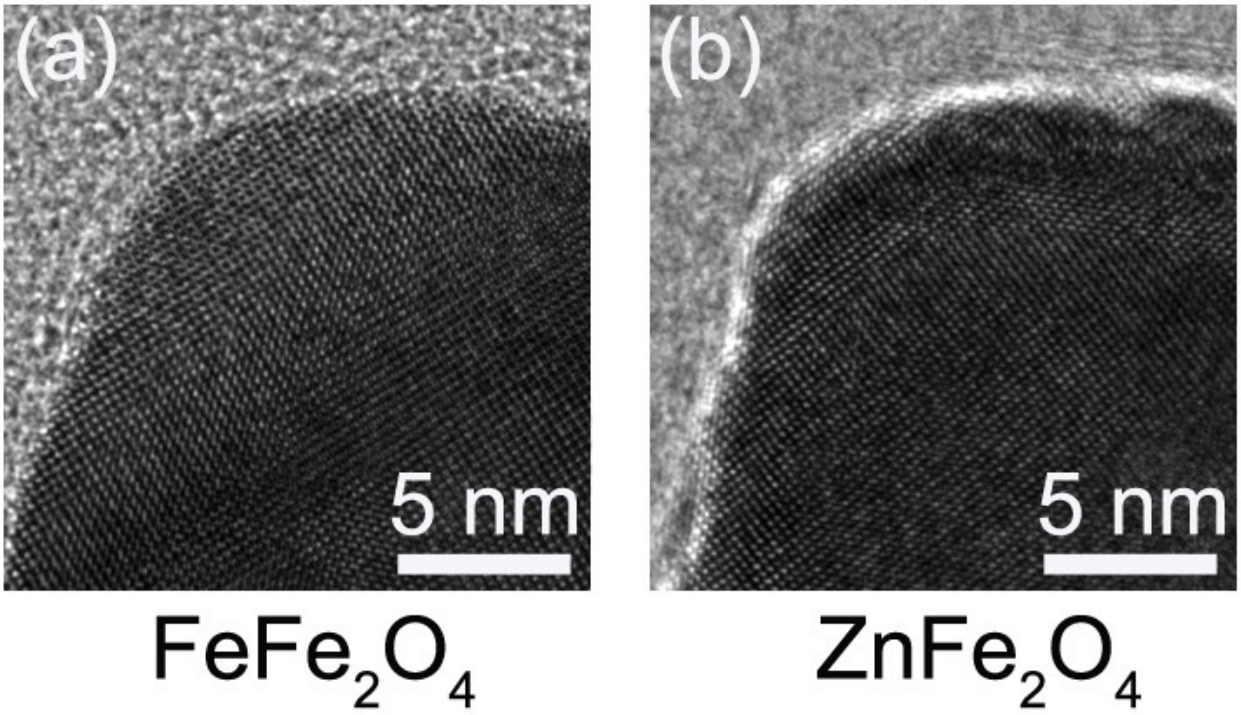

Figure S6. HR-TEM analysis of $FeFe_2O_4$ (a) and $ZnFe_2O_4$ (b) after oxygen evolution reaction (OER).

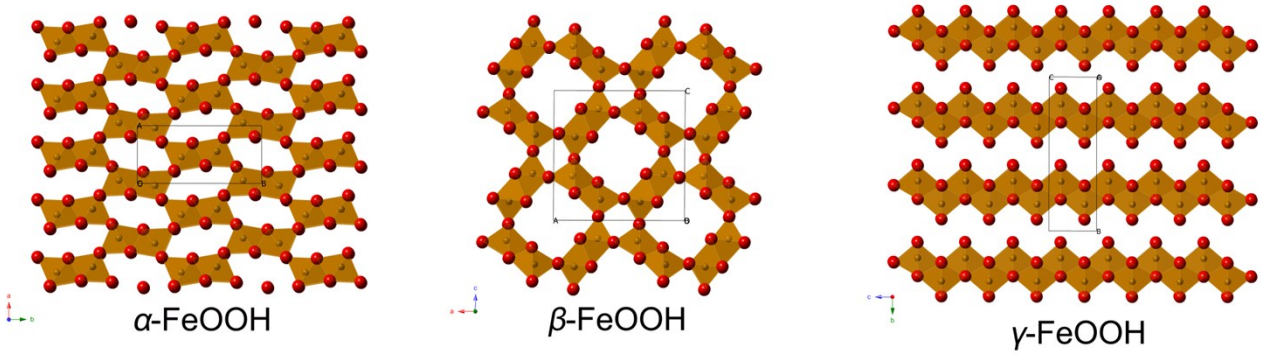

Figure S7. A ball and polyhedrons representation of the crystal structures of *α*-,*β*- and *γ*-FeOOH.

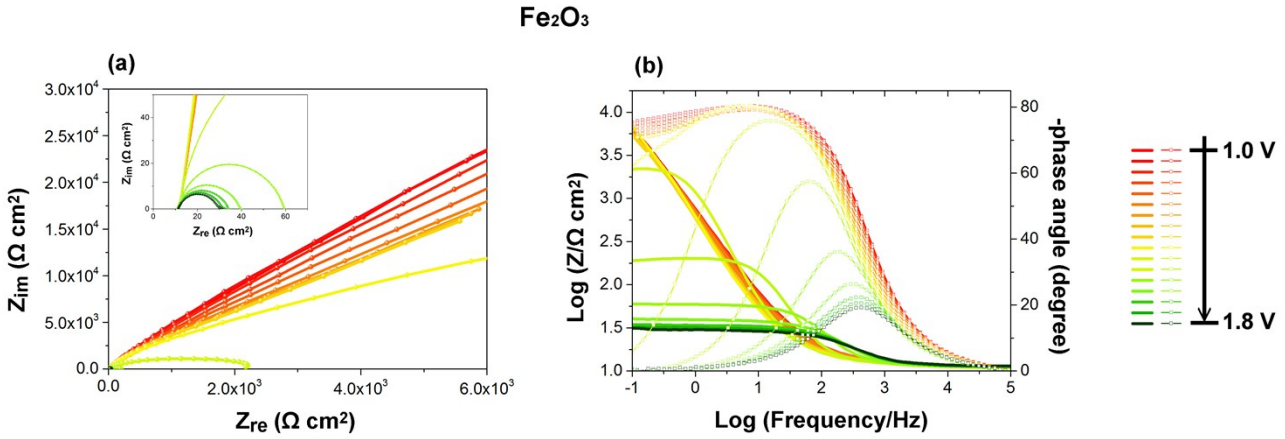

Figure S8. Electrochemical impedance spectra of Fe_2O_3 present Nyquist (a) and Bode (b) plots.

Table S1. Optimum fitting parameters of impedance spectra for $CoFe_2O_4$ sample with a potential range from 1.0 to 1.8 V vs RHE.

potential (vs RHE)	C_{dl} (mF cm^{-2})	R_p (Ω cm^2)	C_{sM} (mF cm^{-2})	R_{sM} (Ω cm^2)	$C_{electroca.}$ (mF cm^{-2})	$R_{electroca.}$ (Ω cm^2)
1.00	2.55×10^{-1}	3.03×10^{6}	2.45×10^{-9}	6.49×10^{0}	6.46×10^{-2}	9.50×10^{4}
1.05	2.63×10^{-1}	5.34×10^{5}	4.05×10^{-9}	5.89×10^{0}	7.96×10^{-2}	5.68×10^{4}
1.10	2.03×10^{-1}	8.91×10^{4}	6.42×10^{-9}	5.65×10^{0}	6.97×10^{-2}	2.11×10^{4}
1.15	2.20×10^{-1}	1.32×10^{4}	7.58×10^{-9}	4.39×10^{0}	1.22×10^{-1}	7.10×10^{4}
1.20	2.38×10^{-1}	7.32×10^{3}	1.19×10^{-8}	3.95×10^{0}	1.01×10^{-1}	1.00×10^{4}
1.25	2.81×10^{-1}	3.90×10^{3}	3.55×10^{-8}	3.02×10^{0}	1.43×10^{-1}	7.04×10^{3}
1.30	3.88×10^{-1}	1.93×10^{3}	5.44×10^{-8}	2.95×10^{0}	2.31×10^{-1}	5.04×10^{3}
1.35	5.88×10^{-1}	8.65×10^{2}	8.32×10^{-8}	1.35×10^{0}	4.64×10^{-1}	4.89×10^{3}
1.40	1.12×10^{0}	2.69×10^{2}	1.65×10^{-7}	1.20×10^{0}	9.15×10^{-1}	2.30×10^{3}
1.45	2.20×10^{0}	9.50×10^{1}	9.08×10^{-1}	9.10×10^{4}	1.00×10^{0}	1.10×10^{3}
1.50	4.23×10^{0}	5.81×10^{1}	4.25×10^{0}	6.65×10^{2}	1.00×10^{0}	5.65×10^{2}
1.55	6.23×10^{0}	3.72×10^{1}	8.41×10^{0}	1.06×10^{2}	1.00×10^{0}	2.80×10^{1}
1.60	9.23×10^{0}	2.60×10^{1}	2.10×10^{1}	4.02×10^{1}	1.00×10^{0}	2.46×10^{0}
1.65	1.30×10^{1}	2.17×10^{1}	3.90×10^{1}	2.54×10^{1}	1.00×10^{0}	4.67×10^{-1}
1.70	1.70×10^{1}	1.76×10^{1}	5.00×10^{1}	1.99×10^{1}	1.00×10^{0}	2.65×10^{-1}
1.75	2.30×10^{1}	1.63×10^{1}	5.70×10^{1}	1.77×10^{1}	1.00×10^{0}	5.11×10^{-2}
1.80	3.00×10^{1}	1.53×10^{1}	5.90×10^{1}	1.64×10^{1}	1.00×10^{0}	1.18×10^{-2}

Table S2. Optimum fitting parameters of impedance spectra for $NiFe_2O_4$ sample with a potential range from 1.0 to 1.8 V vs RHE.

potential (vs RHE)	C_{dl} (mF cm^{-2})	R_p (Ω cm^2)	C_{sM} (mF cm^{-2})	R_{sM} (Ω cm^2)	$C_{electroca.}$ (mF cm^{-2})	$R_{electroca.}$ (Ω cm^2)
1.00	1.54×10^{-1}	8.12×10^{4}	8.98×10^{-10}	8.62×10^{0}	6.31×10^{-2}	2.83×10^{4}
1.05	1.44×10^{-1}	6.06×10^{4}	1.15×10^{-9}	6.38×10^{0}	3.67×10^{-2}	1.81×10^{4}
1.10	1.41×10^{-1}	4.98×10^{4}	4.14×10^{-9}	6.65×10^{0}	3.51×10^{-2}	1.16×10^{4}
1.15	1.45×10^{-1}	5.10×10^{4}	3.69×10^{-9}	4.65×10^{0}	3.87×10^{-2}	5.93×10^{3}
1.20	1.50×10^{-1}	1.31×10^{4}	7.57×10^{-9}	2.39×10^{0}	4.73×10^{-2}	2.22×10^{3}
1.25	1.70×10^{-1}	1.58×10^{3}	8.63×10^{-9}	1.62×10^{0}	3.39×10^{-1}	1.43×10^{3}
1.30	3.27×10^{-1}	3.45×10^{2}	1.94×10^{-8}	1.41×10^{0}	6.20×10^{-2}	2.84×10^{2}
1.35	8.00×10^{-1}	2.23×10^{2}	5.00×10^{-8}	1.16×10^{0}	3.92×10^{-1}	2.61×10^{2}
1.40	1.28×10^{0}	1.95×10^{2}	1.04×10^{-7}	1.04×10^{0}	6.57×10^{-1}	2.08×10^{2}
1.45	1.24×10^{0}	2.03×10^{2}	1.29×10^{0}	2.93×10^{4}	1.99×10^{-1}	1.63×10^{2}
1.50	1.08×10^{0}	1.43×10^{2}	3.45×10^{0}	4.61×10^{2}	1.78×10^{-1}	1.57×10^{2}
1.55	1.54×10^{0}	6.49×10^{1}	9.23×10^{0}	1.08×10^{2}	1.78×10^{-1}	4.54×10^{1}
1.60	3.72×10^{0}	3.15×10^{1}	1.20×10^{1}	4.40×10^{1}	1.78×10^{-1}	1.51×10^{1}
1.65	6.44×10^{0}	2.36×10^{1}	2.40×10^{1}	2.98×10^{1}	1.78×10^{-1}	8.72×10^{0}
1.70	7.83×10^{0}	2.12×10^{1}	3.30×10^{1}	2.52×10^{1}	1.78×10^{-1}	6.38×10^{0}
1.75	9.84×10^{0}	2.09×10^{1}	4.30×10^{1}	2.36×10^{1}	1.78×10^{-1}	5.11×10^{0}
1.80	1.50×10^{1}	1.90×10^{1}	4.70×10^{1}	2.11×10^{1}	1.78×10^{-1}	5.01×10^{0}

Table S3. Optimum fitting parameters of impedance spectra for Fe_3O_4 sample with a potential range from 1.0 to 1.8 V vs RHE.

potential (vs RHE)	C_{dl} (mF cm^{-2})	R_p (Ω cm^2)	C_{sM} (mF cm^{-2})	R_{sM} (Ω cm^2)	$C_{electroca.}$ (mF cm^{-2})	$R_{electroca.}$ (Ω cm^2)
1.00	8.26×10^{-2}	3.29×10^{5}	2.46×10^{-10}	1.24×10^{1}	3.20×10^{-1}	2.94×10^{3}
1.05	8.30×10^{-2}	2.88×10^{5}	3.49×10^{-10}	1.20×10^{1}	3.24×10^{-1}	1.71×10^{3}
1.10	8.73×10^{-2}	2.63×10^{5}	4.81×10^{-10}	1.04×10^{1}	3.27×10^{-1}	1.66×10^{3}
1.15	9.28×10^{-2}	2.61×10^{5}	4.99×10^{-10}	9.44×10^{0}	3.36×10^{-1}	1.64×10^{3}
1.20	9.69×10^{-2}	2.26×10^{5}	5.03×10^{-10}	8.70×10^{0}	3.41×10^{-1}	1.47×10^{3}
1.25	1.00×10^{-1}	2.18×10^{5}	7.45×10^{-10}	8.02×10^{0}	3.52×10^{-1}	1.38×10^{3}
1.30	1.03×10^{-1}	1.98×10^{5}	8.52×10^{-10}	7.63×10^{0}	3.64×10^{-1}	1.29×10^{3}
1.35	1.07×10^{-1}	1.88×10^{5}	8.66×10^{-10}	6.51×10^{0}	3.84×10^{-1}	1.10×10^{3}
1.40	1.12×10^{-1}	1.67×10^{5}	9.08×10^{-10}	6.46×10^{0}	4.00×10^{-1}	8.85×10^{2}
1.45	1.18×10^{-1}	6.5×10^{4}	9.53×10^{-10}	4.85×10^{0}	4.16×10^{-1}	7.85×10^{2}
1.50	1.19×10^{-1}	2.45×10^{3}	9.86×10^{-10}	4.27×10^{0}	4.59×10^{-1}	6.30×10^{2}
1.55	1.69×10^{-1}	7.11×10^{1}	1.14×10^{-9}	2.43×10^{0}	7.66×10^{-1}	2.20×10^{2}
1.60	3.55×10^{-1}	4.28×10^{0}	1.35×10^{-9}	8.15×10^{-1}	2.69×10^{0}	5.30×10^{1}
1.65	8.02×10^{-1}	2.91×10^{0}	4.87×10^{-9}	5.91×10^{-1}	8.60×10^{0}	3.08×10^{1}
1.70	1.27×10^{0}	1.54×10^{0}	1.05×10^{-8}	3.54×10^{-1}	1.00×10^{0}	2.60×10^{1}
1.75	2.91×10^{0}	1.38×10^{0}	1.25×10^{-8}	8.10×10^{-2}	1.60×10^{0}	2.45×10^{1}
1.80	2.05×10^{0}	1.07×10^{0}	2.91×10^{-8}	6.80×10^{-3}	2.10×10^{0}	2.36×10^{1}

Table S4. Optimum fitting parameters of impedance spectra for $ZnFe_2O_4$ sample with a potential range from 1.0 to 1.8 V vs RHE

potential (vs RHE)	C_{dl} (mF cm^{-2})	R_p (Ω cm^2)	C_{sM} (mF cm^{-2})	R_{sM} (Ω cm^2)	$C_{electroca.}$ (mF cm^{-2})	$R_{electroca.}$ (Ω cm^2)
1.00	3.57×10^{-2}	3.80×10^{5}	3.87×10^{-11}	3.52×10^{0}	1.42×10^{-1}	5.89×10^{3}
1.05	3.61×10^{-2}	3.30×10^{5}	6.28×10^{-11}	3.32×10^{0}	1.38×10^{-1}	5.30×10^{3}
1.10	3.72×10^{-2}	3.15×10^{5}	1.69×10^{-10}	2.61×10^{0}	1.37×10^{-1}	5.17×10^{3}
1.15	3.83×10^{-2}	2.91×10^{5}	4.59×10^{-10}	2.02×10^{0}	1.39×10^{-1}	4.82×10^{3}
1.20	3.94×10^{-2}	2.51×10^{5}	1.73×10^{-9}	1.92×10^{0}	1.44×10^{-1}	4.38×10^{3}
1.25	4.02×10^{-2}	2.18×10^{5}	2.07×10^{-9}	1.87×10^{0}	1.49×10^{-1}	3.92×10^{3}
1.30	4.11×10^{-2}	1.92×10^{5}	2.61×10^{-9}	1.72×10^{0}	1.53×10^{-1}	3.76×10^{3}
1.35	4.19×10^{-2}	1.67×10^{5}	3.57×10^{-9}	1.68×10^{0}	1.57×10^{-1}	3.55×10^{3}
1.40	4.25×10^{-2}	1.40×10^{5}	4.51×10^{-9}	1.54×10^{0}	1.61×10^{-1}	3.10×10^{3}
1.45	4.38×10^{-2}	1.06×10^{5}	6.53×10^{-9}	1.51×10^{0}	1.64×10^{-1}	3.05×10^{3}
1.50	4.54×10^{-2}	2.15×10^{4}	6.70×10^{-9}	1.49×10^{0}	1.64×10^{-1}	2.92×10^{3}
1.55	5.47×10^{-2}	3.43×10^{3}	6.83×10^{-9}	1.48×10^{0}	1.63×10^{-1}	2.04×10^{3}
1.60	5.86×10^{-2}	1.16×10^{3}	5.76×10^{-8}	1.47×10^{0}	1.63×10^{-1}	6.89×10^{2}
1.65	8.90×10^{-2}	1.19×10^{2}	1.58×10^{-7}	1.06×10^{0}	1.80×10^{-1}	6.67×10^{2}
1.70	1.18×10^{-2}	3.75×10^{1}	2.03×10^{-7}	6.49×10^{-1}	2.38×10^{-1}	2.99×10^{2}
1.75	1.14×10^{-2}	2.23×10^{1}	2.58×10^{-7}	8.20×10^{-2}	3.55×10^{-1}	1.80×10^{2}
1.80	1.21×10^{-2}	2.68×10^{1}	2.98×10^{-7}	1.42×10^{-2}	4.00×10^{-1}	1.50×10^{2}

Table S5. Optimum fitting parameters of impedance spectra for Fe_2O_3 sample with a potential range from 1.0 to 1.8 V vs RHE

potential (vs RHE)	C_{dl} (mF cm^{-2})	R_p (Ω cm^2)	C_{sM} (mF cm^{-2})	R_{sM} (Ω cm^2)	$C_{electroca.}$ (mF cm^{-2})	$R_{electroca.}$ (Ω cm^2)
1.00	6.04×10^{-2}	4.35×10^{5}	2.22×10^{-10}	1.71×10^{1}	2.64×10^{-1}	5.29×10^{3}
1.05	6.14×10^{-2}	4.19×10^{5}	3.16×10^{-10}	1.66×10^{1}	2.63×10^{-1}	4.81×10^{3}
1.10	6.41×10^{-2}	3.63×10^{5}	7.18×10^{-10}	1.63×10^{1}	2.77×10^{-1}	3.53×10^{3}
1.15	6.85×10^{-2}	3.05×10^{5}	9.34×10^{-10}	1.59×10^{1}	2.92×10^{-1}	2.97×10^{3}
1.20	7.30×10^{-2}	2.70×10^{5}	9.85×10^{-10}	1.47×10^{1}	3.16×10^{-1}	2.08×10^{3}
1.25	7.98×10^{-2}	2.24×10^{5}	1.14×10^{-9}	1.37×10^{1}	3.34×10^{-1}	1.69×10^{3}
1.30	8.43×10^{-2}	1.94×10^{5}	1.18×10^{-9}	1.34×10^{1}	3.56×10^{-1}	1.24×10^{3}
1.35	8.61×10^{-2}	1.77×10^{5}	1.22×10^{-9}	1.27×10^{1}	3.66×10^{-1}	1.02×10^{3}
1.40	9.04×10^{-2}	1.72×10^{5}	1.31×10^{-9}	1.19×10^{1}	3.79×10^{-1}	9.60×10^{3}
1.45	9.60×10^{-2}	5.82×10^{4}	2.66×10^{-9}	9.73×10^{0}	4.01×10^{-1}	9.09×10^{3}
1.50	1.13×10^{-1}	1.19×10^{3}	4.25×10^{-9}	9.29×10^{0}	4.61×10^{-1}	2.24×10^{3}
1.55	2.12×10^{-1}	3.70×10^{1}	3.40×10^{-9}	5.54×10^{0}	8.09×10^{-1}	1.99×10^{2}
1.60	2.80×10^{-1}	5.99×10^{0}	5.97×10^{-9}	3.55×10^{-1}	2.75×10^{0}	5.91×10^{1}
1.65	4.27×10^{-1}	1.72×10^{0}	2.17×10^{-9}	3.59×10^{-1}	5.40×10^{0}	3.95×10^{1}
1.70	4.68×10^{-1}	1.81×10^{0}	4.13×10^{-9}	7.50×10^{-2}	8.18×10^{0}	3.40×10^{1}
1.75	4.61×10^{-1}	1.30×10^{0}	6.98×10^{-9}	8.00×10^{-2}	9.18×10^{0}	3.20×10^{1}
1.80	4.21×10^{-1}	1.32×10^{0}	8.4×10^{-9}	2.29×10^{-2}	1.10×10^{1}	3.03×10^{1}